CYCLE-GAN BASED FEATURE TRANSLATION FOR OPTICAL-SAR DATA IN BURNED AREA MAPPING

E. Çolak, F. Sunar

ITU, Civil Engineering Faculty, Geomatics Engineering Department, 34469 Maslak Istanbul, Turkiye
(colakem, fsunar)@itu.edu.tr

KEY WORDS: Deep Learning, Cycle-GAN, Image Translation, Sentinel-2, Sentinel-1, Forest Fire Burned Area Mapping

ABSTRACT:

For the management of the forest and the assessment of impacts on ecosystems, post-fire burned area mapping is crucial for sustainable environment and forestry. While optical remote sensing data has been extensively used for monitoring forest fires due to its spatial and temporal resolutions, it is susceptible to limitations imposed by poor weather conditions. To overcome this challenge, the complementary use of optical and Synthetic Aperture Radar (SAR) data is beneficial, as SAR can penetrate clouds and capture images in all-weather conditions. However, SAR lacks the necessary spectral features for comprehensive forest fire monitoring and burned area mapping. To overcome these limitations, this study proposes a Cycle-Consistent Generative Adversarial Networks (Cycle-GAN) based deep feature translation method for burned area mapping by combining optical and SAR data. This approach allows for the retrieval of precise information of interest with a level of precision that cannot be achieved by either optical or SAR data alone. The Cycle-GAN uses a cyclic structure to transfer data from one domain (optical) to another domain (SAR) into the same feature space. As a result, it can maintain its spectral characteristics while providing ongoing and current information for monitoring forest fires. For this purpose, Burn Area Index (BAI), Mid Infrared Burn Index (MIRBI), Normalised Burn Ratio (NBR) were determined using optical data and image translation was performed with Cycle-GAN on SAR data. The accuracy of the fake BAI, MIRBI and NBR spectral burn indices determined from the SAR was established by correlating the original spectral burn indices determined from the optical data. The results demonstrate a significant correlation between the real and generated fake burn indices, particularly with a noteworthy correlation coefficient of 0.93 observed for the NBR index. In addition, the findings validate the effectiveness of the generated indices in accurately representing and quantifying the extent of burned areas.

1. INTRODUCTION

Forest ecosystems are currently facing threats due to natural and human-induced degradation associated with global climate change. These risks include forest fires, insect outbreaks, frosts, and diseases, all of which impact the dynamics of forest ecosystems. Among these hazards, forest fires pose the greatest risk, causing extensive damage to trees. Fires, being a frequent and widespread disturbance, have adverse effects on the environment, economy, and society as a whole. They not only harm individual trees but also alter the structure, composition of vegetation, and biogeochemical cycles of the entire forest ecosystem (Sunar and Özkan, 2001; Chaparro et al. 2016; Chowdhury et al., 2015; Çolak and Sunar, 2020a and 2020b).

The mapping of burned areas following a fire is an essential tool for comprehending fire propagation, restoring fire regimes, and effectively managing forest fires. Among various post-fire applications, the utilization of optical remote sensing data has garnered significant attention, particularly in the context of burn area mapping. The diverse spatial and temporal resolutions of optical remote sensing data enable accurate depiction of Earth features' texture, geometric shape, and spectral information, thereby facilitating precise burned area mapping. Several spectral indices, formed by mathematical combinations or transformations of optical spectral bands, serve as valuable tools for mapping burned areas. These indices are indispensable for accurately delineating burned regions, as they can differentiate between distinct vegetation types and burned areas based on their unique reflectance properties. Consequently, they contribute to a precise assessment of the extent and severity of forest fires. Nevertheless, the inherent susceptibility of optical data to weather conditions poses a challenge in promptly acquiring post-fire data, thereby impeding an accurate assessment of the initial aftermath and effective fire management (Gonçalves and Sousa, 2017; Çolak and Sunar, 2022).

On the other hand, Synthetic Aperture Radar (SAR) data offer the advantage of capturing ground surface scattering information regardless of weather conditions, making it a valuable tool for mapping fire-affected regions. SAR's ability to penetrate clouds further enhances its utility in this context. Nonetheless, the precision of SAR results may not always match those obtained through optical remote sensing, as the optical spectral indices enable a more precise assessment of forestry dynamics by providing essential spectral information for monitoring the phenological stages of forests. Consequently, the simultaneous processing of temporal sequences from optical and radar sources enables the retrieval of valuable information with an enhanced precision that surpasses the capabilities of each individual modality when used independently (Şener et al., 2021; Çolak and Sunar, 2022).

In recent years, the utilization of deep learning algorithms has witnessed a notable surge in the field of remote sensing applications. Specifically, these algorithms have gained traction for their ability to perform feature translation tasks, aimed at leveraging the complementary information extracted from both optical and radar data sources, thereby enabling a more comprehensive understanding of the Earth's surface and its dynamic processes. Among the various approaches in this domain, the Cycle-Consistent Generative Adversarial Networks (Cycle-GAN) method has garnered significant attention. By employing a cyclic architecture, Cycle-GAN facilitates the seamless transformation of images from the optical domain to

the synthetic aperture radar (SAR) domain, aligning them harmoniously within a shared feature space. This innovative technique holds great promise for advancing the capabilities of remote sensing technologies, with diverse potential applications ranging from land cover classification and change detection to disaster monitoring and environmental assessment (Liu and Lei, 2018; Huang et al., 2019; Wang et al. 2019; Çolak and Sunar, 2022).

The proposed method involves the integration of optical and SAR data through deep feature translation techniques, enabling the extraction and incorporation of valuable information from both modalities. By combining the complementary strengths of optical and SAR data, the proposed approach aims to enhance the accuracy and effectiveness of burned area mapping.

To accomplish this objective, the study utilized optical data to calculate the Burn Area Index (BAI), Mid Infrared Burn Index (MIRBI), and Normalised Burn Ratio (NBR). Additionally, the Cycle-GAN technique was employed to perform image translation on SAR data. The accuracy of the resultant synthetic/fake BAI, MIRBI, and NBR spectral burn indices derived from the SAR data was determined by establishing correlations with the original spectral burn indices obtained from the optical data.

2. STUDY AREA

The forest fire took place in the Menderes district which is within the border of Izmir Forestry Chief Directorate (IFCD) located in the Aegean region of Türkiye (Figure 1).
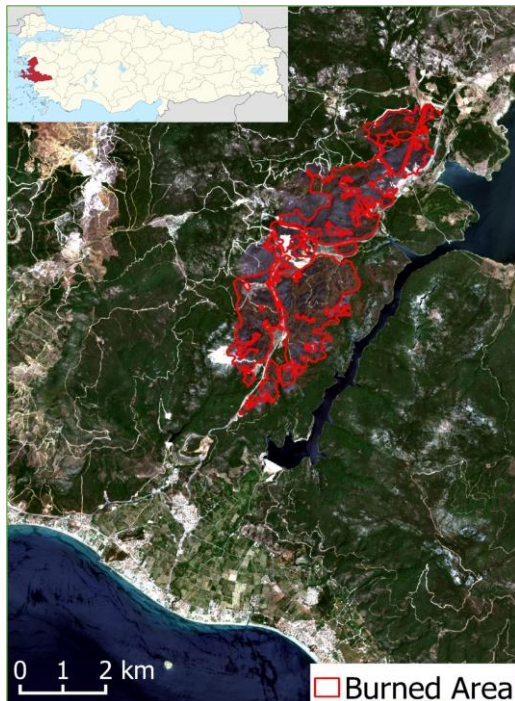
Figure 1. Study area.

The fire started on July 1, 2017 in maquis forest area and continued for 4 days, and extinguished on July 5, 2017. According to field measurements conducted by the IFCD, the fire caused damage to approximately 986 ha of forest area.

3. DATA COLLECTION

The analysis utilized Sentinel-1 and Sentinel-2 datasets, with their inherent characteristics provided in Table 1 for reference.

Mission	Sensors	Temporal resolution (day)	Spatial resolution (m)
Sentinel 1	C - Band SAR	12	(SM) & (IW) 10 x 10 (EW) 25 x 25
Sentinel 2	Multispectral Instrument (MSI)	10	10, 20 & 60

Table 1. The characteristics of Sentinel-1 and -2 data (Soille et al., 2016).

To overcome the challenge of identifying burned forest areas under cloud cover, Sentinel-1 data was utilized as an alternative feature. Through the application of Cycle-GAN-based feature translation, the most suitable dataset was determined for post-fire imagery. Specifically, the dates 17th and 18th July 2017 were identified as the optimal post-fire dates for Sentinel-2 and Sentinel-1, respectively.

4. METHODOLOGY

In this study, various image-processing steps and analysis such as pre-processing, spectral indices, deep feature translation, statistical analysis, and burned area mapping were applied (Figure 2).
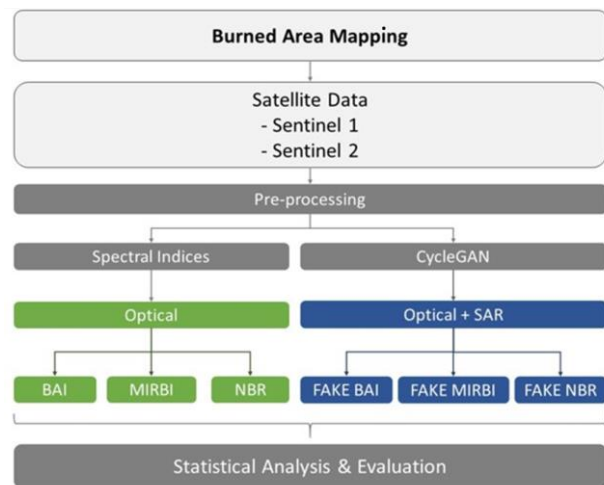
Figure 2. Flow chart of the study.

4.1. Spectral Burn Indices

Spectral burn indices utilize numerical values that represent brightness across multiple bands and can be effectively used in mathematical operations to extract relevant information related to specific target features. In this study, spectral burn indices were employed to assess the extent of burned areas in the post-fire stage. These indices leverage the spectral response of different bands to quantify the changes in vegetation and surface conditions caused by fire, enabling a quantitative evaluation of the fire's impact on the landscape.

Three spectral burn indices were employed in this study:
- The BAI is primarily used to identify and improve the burned (char) signal. It calculates the spectral distance in red near infrared (R-NIR) bi-spectral space from each pixel to the combination of burned pixels as a reference point.
- The NBR was created with the particular purpose of extracting burned areas and assessing burn severity. It utilizes the Shortwave Infrared (SWIR) and Near Infrared (NIR) bands.
- The MIRBI is specifically developed for shrub ecosystems. It combines two Short-Wave Infrared (SWIR) bands that offer improved discrimination in burned areas, making it well-suited for assessing fire impacts on shrub vegetation (Colak and Sunar, 2020c).

Table 2 provides an overview of the various spectral indices employed in this study.

Index	Formula	Interpretation
BAI	$BAI = \dfrac{1}{(0.1 - Red)^2 + (0.06 - NIR)^2}$	It emphasizes the charcoal signal in post-fire images.
NBR	$MIRBI = 10 \times LSWIR - 9.8 \times SSWIR + 2$	It combines two SWIR bands due to their better separation in burned areas.
MIRBI	$NBR = \dfrac{(NIR - SWIR)}{(NIR + SWIR)}$	It is designed for burned area extraction.
NIR: Near-Infrared SWIR: Shortwave Infrared LSWIR: Long Shortwave Infrared SSWIR: Short Shortwave Infrared		

Table 2. Spectral burn indices used.

4.2. Cycle-Consistent Generative Adversarial Networks (Cycle-GAN)

Generative Adversarial Networks (GANs), as established models of probability generation, possess the ability to discern the internal distribution of data through extensive learning from large datasets. GANs employ an unsupervised deep learning approach for image generation, effectively generating data. In essence, GANs consist of two networks, namely the generator and the discriminator, working in tandem to produce new images. The Cycle-GAN, which is a specific variant of the Generative Adversarial Network (GAN) model, was developed utilizing a framework incorporating cycle constraints to facilitate image-to-image translations. By enforcing these constraints, the model enables the seamless transformation of images from one domain to another while preserving their inherent characteristics (Liu and Lei, 2018; Wang et al., 2019; Li et al., 2021; Çolak and Sunar, 2022).

Cycle-GANs have demonstrated their efficacy in enhancing performance, particularly in domains including crop type mapping and identification, change detection, and forest fire detection and mapping (Park et al., 2020; Ren et al., 2020; Li et al., 2021; Çolak and Sunar, 2022).

The mathematical formulation of Cycle-GAN is as follows (Eq. 1).

$$L(F, G, D_X, D_Y) = L_{GAN}(F, D_Y) + L_{GAN}(G, D_X) + \lambda L_C(F, G) \quad (1)$$

The notation $L_{GAN}(G, D)$ represents the conventional loss function of a GAN, comprising a generator G and a discriminator D. On the other hand, $L_C(F, G)$ denotes the cycle loss, which is mathematically defined by Eq.2 as follows.

$$L_C(F, G) = \mathbb{E}_{x \sim X}\left[\left\|G(F(X)) - x\right\|_1\right] + \mathbb{E}_{y \sim Y}\left[\left\|F(G(Y)) - y\right\|_1\right] \quad (2)$$

and λ is a hyper-parameter (Wang et al., 2019).

The primary objective of Cycle-GAN in the context of image-to-image translation is to establish a mapping between input and output images by leveraging a training set composed of aligned image pairs, which belongs to the domain of vision and graphics challenges. One of the significant breakthroughs facilitated by GANs in addressing the image-to-image translation challenge is the adoption of a structured loss, which penalizes the global configuration of the output image rather than treating each output pixel in isolation from the rest of the input image (Wang et al., 2019; Chen et al., 2020).

Cycle-GAN is a technique for image-to-image translation that operates without the reliance on paired images. It enables the transformation of images from a given reference image domain (X) to a desired target image domain (Y).

In this study, the images were divided into small patches to create image pairs. A total of 800 image pairs were used for training, while 200 image pairs were reserved for testing purposes.

4.3. Statistical Analysis and Evaluation

Correlation analysis is a simple yet powerful method used to explore the relationship between two variables. In the field of remote sensing, the Pearson's correlation coefficient (R) is a widely utilized statistical measure that quantifies the strength and direction of the linear association between variables. With a numerical value ranging between -1 and 1, the correlation coefficient indicates the direction of the relationship, where a positive value suggests both variables tend to increase together and vice versa for a negative value. Additionally, the magnitude of the coefficient reflects the strength of the linear relationship, with values closer to 1 or -1 indicating a stronger association between the variables.

In the statistical analysis conducted, the Pearson's correlation coefficient method was applied to examine the relationship between the Cycle-GAN-generated fake image and optical-SAR vegetation indices.

For evaluating the results, the areal extent of the burned forest area is calculated, and all results were given spatially and quantitatively.

5. RESULTS AND DISCUSSION

5.1. Spectral Burn Indices

Firstly, the spectral burn indices, namely BAI, NBR, and MIRBI, were derived from data acquired by the Sentinel-2 for post-fire images (Figure 3).
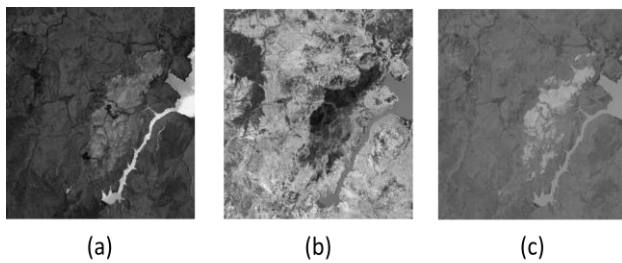
Figure 3. Spectral burn indices; (a) BAI, (b) NBR, and (c) MIRBI.

As depicted in Figure 3, a notable distinction can be observed between the fire-affected areas and the unaffected areas based on the calculated values of the spectral burn indices. This observation highlights the efficacy of these indices in accurately identifying and distinguishing the extent of the burned areas, emphasizing their effectiveness in fire detection and mapping.

5.2. Cycle-GAN

In the initial step, the images underwent a partitioning process into smaller patches, thereby generating image pairs that were subsequently utilized in the application of the Cycle-GAN model (Figure 4). Following this, the designated datasets were processed using the Cycle-GAN method, utilizing the specified feature inputs as indicated.
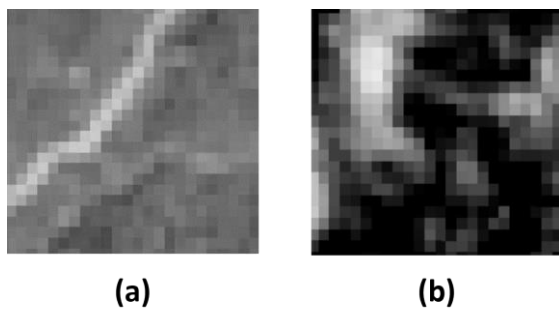
Figure 4. Example of image pairs for training and test; (a) Optical, and (b) SAR.

As shown in Figure 5, the application of the Cycle-GAN method yielded highly successful outcomes. The generated fake burn indices closely resemble the real burn indices, demonstrating the effectiveness of the image-to-image translation process. The spatial comparison between the real and generated fake burn indices reveals minimal differences, indicating the ability of the Cycle-GAN model to accurately capture and reproduce the spectral characteristics of burned areas.

5.3. Statistical Analysis and Evaluation

A correlation study was conducted to assess the strength of the relationship between the real and generated spectral burn indices, employing the Pearson correlation coefficient as a measure of correlation (Table 3).
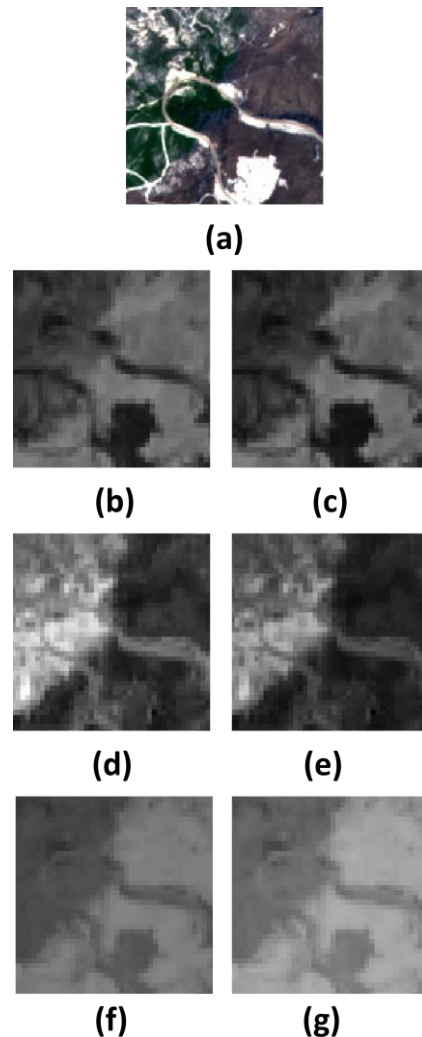
Figure 5. Real and fake spectral indices generated by Cycle-GAN; (a) Original optical data, (b) Real BAI, (c) Fake BAI, (d) Real NBR, (e) Fake NBR, (f) Real MIRBI, and (g) Fake MIRBI.

Correlation Analysis	R
BAI – Fake BAI	0.78
NBR – Fake NBR	0.93
MIRBI – Fake MIRBI	0.69

Table 3. Correlation analysis between real and fake burn indices.

The findings of the study revealed a strong correlation between the real and generated burn indices, particularly with a high correlation coefficient of 0.93 observed between the real and fake NBR. This substantial correlation highlights the remarkable success of the Cycle-GAN-generated burn indices in accurately capturing the spectral characteristics of burned areas. These results affirm the spatial and quantitative accuracy achieved by the Cycle-GAN method in generating synthetic burn indices that closely resemble the real data.

Furthermore, to quantitatively assess the similarity between the real and generated spectral index results, the extent of the burned forest area was calculated in both maps. This direct comparison allowed for an objective evaluation of the accuracy and reliability of the generated maps in representing the burned forest area (Table 4).

	Real BAI	Fake BAI	Real NBR	Fake NBR	Real MIRBI	Fake MIRBI
Burned Area (ha)	997	999	991	988	853	846
According to the IFCD (ha)	986					

Table 4. Areal extent of the burned area.

Based on field measurements conducted by the IFCD, the areal extent of the burned forest area was determined to be 986 ha. The comparison of the calculated extents confirmed a close agreement between the real and generated spectral index outcomes, further reinforcing the accuracy of the generated maps in accurately representing the burned forest area. However, it should be noted that the MIRBI indexes yielded lower estimates of the burned area for both real and fake images, indicating a different sensitivity to fire-induced changes in vegetation and surface reflectance compared to the BAI and NBR indices.

6. CONCLUSION

This study highlights the capability of deep learning techniques to extract valuable information from optical and SAR data, encompassing spectral features, roughness, moisture, biomass, vegetation structure, and height. Through the application of deep learning, particularly the Cycle-GAN method, image translation from the optical to the desired SAR domain becomes possible, generating synthetic burn indices with remarkable spatial accuracy and quantitative metrics. Moreover, these deep learning techniques address the constraints of traditional remote sensing data, allowing for continuous and up-to-date information, thus enhancing the analysis and monitoring of burned areas.

The findings of the study demonstrate a significant correlation between the real and generated fake burn indices, with a noteworthy correlation coefficient of 0.93 observed in the case of the NBR. In order to further evaluate the similarity between the real and generated spectral index outputs, a quantitative assessment was conducted by calculating the areal extent of the burned forest area in both sets of maps. Impressively, a high level of similarity was observed between the field measurements and the calculated burned forest area in the generated maps, with a remarkable 99.8% similarity between the field measurements and the fake NBR. These compelling results provide strong evidence for the accuracy and reliability of the generated spectral indices in effectively representing and quantifying the extent of the burned forest area. Additionally, the strong agreement between the real and generated fake indices reinforces the potential of deep learning techniques to effectively bridge the domain gap between optical and SAR data, enabling comprehensive analysis and monitoring of burned areas with improved spatial accuracy and quantitative metrics. However, it is important to note that further testing and evaluation of this technique in different forest fire scenarios is necessary to validate the method's generalization and applicability in diverse forest ecosystems.

As a future plan, it is worth considering the exploration of alternative Generative Adversarial Networks (GANs) methods, such as Pix2Pix and StarGAN, for the fusion of optical and SAR data. These GANs methods have shown promise in image translation tasks and can potentially enhance the analysis and interpretation of diverse data sources. By incorporating these alternative GANs methods into research and development efforts, we can further expand the range of techniques available for leveraging data diversity and redundancy. This exploration will not only contribute to forest fire applications but also facilitate the utilization of multi-sensor data for various fields, including environmental monitoring, disaster management, and beyond.

REFERENCES

Chaparro, D., Vall-Llossera, M., Piles, M., Camps, A., Rüdiger, C., Riera-Tatché, R., 2016. Predicting the extent of wildfires using remotely sensed soil moisture and temperature trends. *IEEE Journal of Selected Topics in Applied Earth Observations and Remote Sensing*, 9(6), 2818-2829.

Chen, J., Wang, L., Feng, R., Liu, P., Han, W., Chen, X., 2020. CycleGAN-STF: Spatiotemporal fusion via CycleGAN-based image generation. *IEEE Transactions on Geoscience and Remote Sensing*, 59(7), 5851-5865.

Chowdhury, E.H., Hassan, Q.K., 2015. Operational perspective of remote sensing-based forest fire danger forecasting systems. *ISPRS Journal of Photogrammetry and Remote Sensing*, 104, 224-236.

Çolak, E., Sunar, F., 2020a. The importance of ground-truth and crowdsourcing data for the statistical and spatial analyses of the NASA FIRMS active fires in the Mediterranean Turkish forests. *Remote Sensing Applications: Society and Environment*, 19, 100327.

Çolak, E., Sunar, F., 2020b. Evaluation of forest fire risk in the Mediterranean Turkish forests: A case study of Menderes region, Izmir. *International journal of disaster risk reduction*, 45, 101479.

Çolak, E., Sunar, F., 2020c. Spatial pattern analysis of post-fire damages in the Menderes district of Turkey. *Frontiers of Earth Science*, 14, 446-461.

Çolak, E., Sunar, F., 2022. A comparison between Cycle-Gan based feature translation and optical-SAR vegetation indices. The International Archives of Photogrammetry, Remote Sensing and Spatial Information Sciences, 43, 583-588.

Gonçalves, A.C., Sousa, A.M., 2017. The fire in the Mediterranean region: A case study of forest fires in Portugal. Mediterranean Identities-Environment, Society, Culture; Fuerst-Bielis, B., Ed, 305-335.

Huang, X., Wen, L., Ding, J., 2019. SAR and optical image registration method based on improved CycleGAN. 6th Asia-Pacific Conference on Synthetic Aperture Radar (APSAR), IEEE, (pp. 1-6).

Li, X., Du, Z., Huang, Y., Tan, Z., 2021. A deep translation (GAN) based change detection network for optical and SAR remote sensing images. *ISPRS Journal of Photogrammetry and Remote Sensing*, 179, 14-34.

Liu, L., Lei, B., 2018. Can SAR images and optical images transfer with each other?. In IGARSS 2018 - 2018 IEEE International Geoscience and Remote Sensing Symposium, (pp. 7019-7022).

Park, M., Tran, D.Q., Jung, D., Park, S., 2020. Wildfire-detection method using DenseNet and CycleGAN data augmentation-based remote camera imagery. *Remote Sensing*, 12(22), 3715.

Ren, C.X., Ziemann, A., Theiler, J., Durieux, A.M., 2020. Cycle-consistent adversarial networks for realistic pervasive change generation in remote sensing imagery. In 2020 IEEE Southwest Symposium on Image Analysis and Interpretation (SSIAI) (pp. 42-45).

Soille, P., Burger, A., Rodriguez, D., Syrris, V., Vasilev, V., 2016. March. Towards a JRC earth observation data and processing platform. In Proceedings of the Conference on Big Data from Space (BiDS'16), Santa Cruz de Tenerife (pp. 15-17).

Sunar, F. and Özkan, C., 2001. Forest fire analysis with remote sensing data. *International Journal of Remote Sensing*, *22*(12), pp.2265-2277.

Şener, E., Çolak, E., Erten, E., Taşkin, G., 2021. The added value of Cycle-GAN for agriculture studies. In 2021 IEEE International Geoscience and Remote Sensing Symposium IGARSS (pp. 7039-7042).

Wang, L., Xu, X., Yu, Y., Yang, R., Gui, R., Xu, Z., Pu, F., 2019. SAR-to-optical image translation using supervised cycle-consistent adversarial networks. *IEEE Access*, 7, 129136-129149.